Plasmonic Nanostructures: Artificial Molecules

HUI WANG,[†,‡] DANIEL W. BRANDL,[‡,§] PETER NORDLANDER,[‡,§,⊥] AND NAOMI J. HALAS*[,†,‡,⊥]

Department of Chemistry, Department of Physics and Astronomy, Department of Electrical and Computer Engineering, and the Laboratory for Nanophotonics, Rice University, Houston, Texas 77005

Received June 19, 2006

ABSTRACT

This Account describes a new paradigm for the relationship between the geometry of metallic nanostructures and their optical properties. While the interaction of light with metallic nanoparticles is determined by their collective electronic or plasmon response, a compelling analogy exists between plasmon resonances of metallic nanoparticles and wave functions of simple atoms and molecules. Based on this insight, an entire family of plasmonic nanostructures, *artificial molecules*, has been developed whose optical properties can be understood within this picture: nanoparticles (nanoshells, nanoeggs, nanomatryushkas, nanorice), multinanoparticle assemblies (dimers, trimers, quadrumers), and a nanoparticle-over-metallic film, an electromagnetic analog of the spinless Anderson model.

Introduction

The vivid, beautiful optical properties of nanostructured metals have been known since antiquity, long before our first scientific understanding of the interaction between light and metals. One of the initial achievements of classical electromagnetic theory, in fact, was the theoretical analysis of the interaction of light with tiny gold spheres, predicting their absorption of light in the blue-green region of the spectrum, a property that gives rise to the intense red color of ruby glass.[1] In subsequent decades, there has been a great deal of interest in the role of quantum size effects on the physical properties of metal particles, with a primary focus on how metallic behavior develops with increasing particle size starting from the atomic state.[2]

The optical properties of metallic nanostructures are determined by the collective oscillations of their conduction electrons with respect to the positive ion background, known as plasmons.[3,4] It has recently become apparent that the plasmons of metallic nanostructures, while describable by classical electromagnetic theory, exhibit certain characteristics that are analogous to electrons in quantum systems. This is seen most clearly in complex nanostructures, where plasmons on neighboring structures or surfaces interact, for then the plasmons mix and hybridize just like the electron wave functions of simple atomic and molecular orbitals. This property, one that we have termed "plasmon hybridization", governs the optical properties of metallic nanostructures of increasingly complex geometries, providing the scientist with a powerful and general design principle that can be applied to guide the design of metallic nanostructures and to predict their resonant properties.[5] Although similarities between plasmons in nanostructures and atomic and molecular wave functions have long been a casual observation of workers in this field, it is only recently, when breakthroughs in the controlled chemical fabrication of metallic nanostructures of various shapes and sizes have been combined with powerful computational methods, that this analogy has been realized, verified, and subsequently exploited in the design of complex plasmonic nanostructures.

Plasmon hybridization theory deconstructs a composite nanostructure into more elementary shapes and then calculates how the plasmon resonances of the elementary geometries interact with each other to generate the hybridized plasmon modes of the composite nanostructure. This theory enables scientists to draw on decades of intuition from molecular orbital theory to correctly predict the plasmonic response of complex nanostructures. In this Account, we show how the plasmon hybridization picture has been applied to both predict and analyze the plasmonic properties of metallic nanostructures, *artificial molecules*, of various geometries. The resulting optical properties of plasmonic nanostructures are in many ways complementary to those of semiconductor nanocrystals, quantum dots, frequently referred to as *artificial atoms* because the discrete narrow lines of their light emission spectrum are determined by particle size, a direct manifestation of their particle-in-a-box-like energy states.[6,7]

Hui Wang was born in Nanjing, China. He received his B.S. and M.S. in chemistry from Nanjing University in 2001 and 2003, respectively. He is currently a Ph.D. candidate in physical chemistry working with Naomi J. Halas at Rice University. His research focuses on plasmonic nanostructures and surface-enhanced spectroscopies.

Daniel Brandl was born in Houston, TX. He received his B.S. in physics from the University of North Carolina at Chapel Hill in 2002 and M.S. in physics from Rice University in 2005. He is currently a Ph.D. candidate in physics and astronomy working with Peter Nordlander at Rice University. His research focuses on the theory of plasmon hybridization applied to nanoparticle systems.

Peter Nordlander was born in Stockholm, Sweden. He received his B.S., M.S., and Ph.D. from Chalmers University of Technology in Gothenburg, Sweden. He has held research positions at IBM Thomas J. Watson Research Center, AT&T Bell Laboratories, Vanderbilt University, Rutgers University, and the University of Paris. He is currently Professor of Physics and Astronomy and Professor of Electrical and Computer Engineering at Rice University, where he is a member of the Laboratory for Nanophotonics.

Naomi J. Halas was born in New Eagle, Pennsylvania. She received her B.A. in chemistry from La Salle University in Philadelphia, PA, and her M.A. and Ph.D. in physics from Bryn Mawr College. She was a research fellow at IBM T. J. Watson Research Center throughout her graduate career and a postdoctoral research fellow at AT&T Bell Laboratories. She is currently the Stanley C. Moore Professor of Electrical and Computer Engineering and Professor of Chemistry at Rice University, where she is also the Director of the Laboratory for Nanophotonics.

* Corresponding author. E-mail: halas@rice.edu. Tel: (713) 348-5611. Fax: (713) 348-5686.
† Department of Chemistry.
‡ The Laboratory for Nanophotonics.
§ Department of Physics and Astronomy.
⊥ Department of Electrical and Computer Engineering.

10.1021/ar0401045 CCC: $37.00
Published on Web 09/21/2006

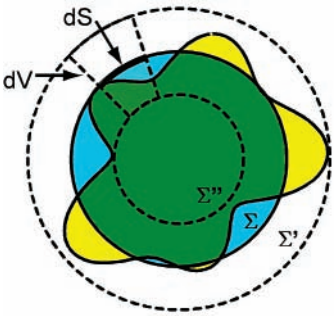

FIGURE 1. Illustration of the incompressible, irrotational fluid of conduction electrons of a finite metallic particle. The surfaces Σ′ and Σ″ are the maximum and minimum boundaries of the fluid, and Σ denotes the nanoparticle boundary.

Our starting point is the nanoshell: a spherical nanoparticle whose optical resonances are determined by the inner and outer radius of its metallic shell layer.[8,9] The unusually sensitive dependence of the optical resonance of a nanoshell on the relative inner and outer shell dimensions provided the initial observation that led to our development of the plasmon hybridization picture. Nanoshells with an offset core, or "nanoeggs", show how the selection rules that govern the mixing of plasmonic states in the nanoshell geometry can be modified under reduced symmetry.[10] The plasmon hybridization picture extends naturally to more complex multilayer nanoshell structures, such as a nanoshell embedded within a nanoshell, or a "nanomatryushka",[5,11] and to prolate spheroidal nanoparticles, or "nanorice".[12] The plasmon resonances of simple ordered assemblies of metallic nanoparticles, for example, nanoparticle dimers, trimers, and quadrumers, where group theory can be applied to classify plasmon modes using the irreducible representations of point groups, exhibit another valuable analogy with molecular orbital theory.[13−15] Finally, the plasmon hybridization picture is applied to the interaction between the localized plasmon resonances of a metallic nanoparticle and the extended propagating surface plasmons of a metallic film.[16] This geometry is the photonic analog of the spinless Anderson−Fano model, which describes phenomena such as chemisorption.

The Incompressible Fluid Model

Plasmon hybridization considers the conduction electrons of a metal to be a charged, incompressible, and irrotational fluid sitting on a rigid, uniform, and positive background charge representing the fixed ion cores (Figure 1). The deformation of the fluid can be expressed in terms of a scalar function, η. Infinitesimal deformations in this fluid give rise to a surface charge density that interacts electrostatically, and plasmons are considered to be the self-sustained oscillations of this electron fluid. The Lagrangian for such a system is

$$L = \frac{n_0 m_e}{2}\int \eta \vec{\nabla}\eta \, dS - \frac{1}{2}\int \frac{\sigma(\vec{r})\sigma(\vec{r}')}{|\vec{r} - \vec{r}'|} dS \, dS', \qquad (1)$$

where n_0 is the electronic density of the conduction electrons, m_e is the mass of an electron, and σ is the surface charge density,

$$\frac{d}{dt}\sigma = n_0 e \frac{d\eta}{d\hat{n}} \qquad (1)$$

and the integrations are performed over all surfaces of the metal. The plasmon modes of the systems are obtained from the Euler−Lagrange equations.

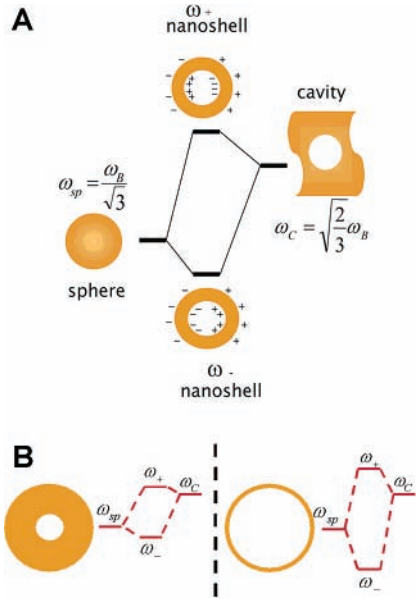

FIGURE 2. Energy level diagrams (A) depicting plasmon hybridization in metal nanoshells resulting from interacting sphere and cavity plasmons with the two hybridized plasmon modes being an antisymmetric or "antibonding" plasmon (ω_+) and a symmetric or "bonding" plasmon resonance (ω_-) and (B) illustrating the dependence of nanoshell plasmon energies on the strength of the interaction between the sphere and cavity plasmons, determined by the thickness of the metallic shell.

Nanoshell Plasmons: The Sphere−Cavity Model

In striking contrast to the plasmonic resonances of solid metallic nanostructures, which exhibit only a weak dependence on particle size or aspect ratio, the plasmon resonances of a nanoshell are a sensitive function of the nanoparticle's inner and outer shell dimensions. While this is a property that can be calculated using electromagnetic theory, it has also recently been verified using *ab initio* quantum mechanical electronic structure methods.[17−20] This convergence between electronic structure and electromagnetic theory provides a prime example of the validity of the plasmon hybridization picture.

The geometry-dependent nanoshell plasmon resonances result from the interaction between the essentially fixed frequency plasmon response of a sphere and that of a cavity (Figure 2A).[5,21] The sphere and cavity plasmons are electromagnetic excitations at the outer and inner interfaces of the metal shell, respectively. Because of the finite thickness of the shell layer, the sphere and cavity plasmons interact with each other and hybridize in a way analogous to the hybridization between atomic orbitals.

As illustrated in Figure 2, this interaction results in the splitting of the plasmon resonances into two new resonances, the lower energy symmetric or "bonding" plasmon (ω_-) and the higher energy antisymmetric or "antibonding" plasmon (ω_+). The strength of the interaction between the sphere and cavity plasmons is controlled by the thickness of the metal shell layer (Figure 2B).

For simplicity, we assume that the conduction electrons form a uniform electron gas of density n_0 with a bulk plasmon frequency $\omega_B = (4\pi e^2 n_0/m_e)^{1/2}$. The cavity plasmon frequency can be expressed as $\omega_{C,l} = \omega_B((l+1)/(2l+1))^{1/2}$ and the sphere plasmon has a vibration frequency $\omega_{S,l} = \omega_B(l/(2l+1))^{1/2}$, where l refers to the multipolar symmetry of the plasmon mode. In a nanoshell, the deformation fields associated with the cavity and sphere plasmons introduce surface charges at both the inner and outer boundaries of the shell. These surface charges couple the sphere and cavity modes, resulting in hybridized plasmons. The hybridization of the cavity and the sphere plasmons depends on the difference in their energies $\omega_{C,l}$ and $\omega_{S,l}$ and on their interaction, which is determined by the thickness of the shell.

To describe the geometry of a nanoshell, we adopt the notation (a,b) to indicate the inner radius a and the outer radius b of the shell. The hybridization between the cavity and sphere plasmons gives rise to two hybridized plasmon modes $|\omega_+\rangle$ and $|\omega_-\rangle$ for each $l > 0$. For a vacuum core, the frequencies of these modes are

$$\omega_{l\pm}^2 = \frac{\omega_B^2}{2}\left\{1 \pm \frac{1}{2l+1}\left[1 + 4l(l+1)\left(\frac{a}{b}\right)^{2l+1}\right]^{1/2}\right\}$$

The $|\omega_+\rangle$ mode corresponds to antisymmetric coupling between the sphere and cavity modes, and the $|\omega_-\rangle$ mode corresponds to symmetric coupling between the two modes. The lower energy $|\omega_-\rangle$ plasmon interacts strongly with the incident optical field, while the $|\omega_+\rangle$ mode interacts weakly and, in the case of Au, is further damped by interband transitions at energies above the d-band to Fermi energy optical transitions at approximately 2.3 eV.

The validity of this expression for the nanoshell plasmon energies has been explicitly verified using fully quantum mechanical calculations.[19,20] Although the resulting plasmon energies are the same as what would be obtained from a Drude dielectric function and classical Mie scattering theory in the nonretarded limit, the present treatment very clearly elucidates the nature of the nanoshell plasmon resonances and, in particular, the microscopic origin of their sensitive dependence on geometry. For example, this picture provides a simple and intuitive explanation for why the energy of the optically active plasmon resonance shifts to lower energies with decreasing shell thickness: the decreased shell thickness leads to a stronger coupling between the sphere and cavity plasmons, increasing the splitting between the bonding and antibonding hybridized plasmons.[21] This result is in quantitative agreement with Mie scattering theory, which offers no such physical picture for this effect.

Several synthetic/fabrication routes have been developed for nanoshells. These include the reduction of

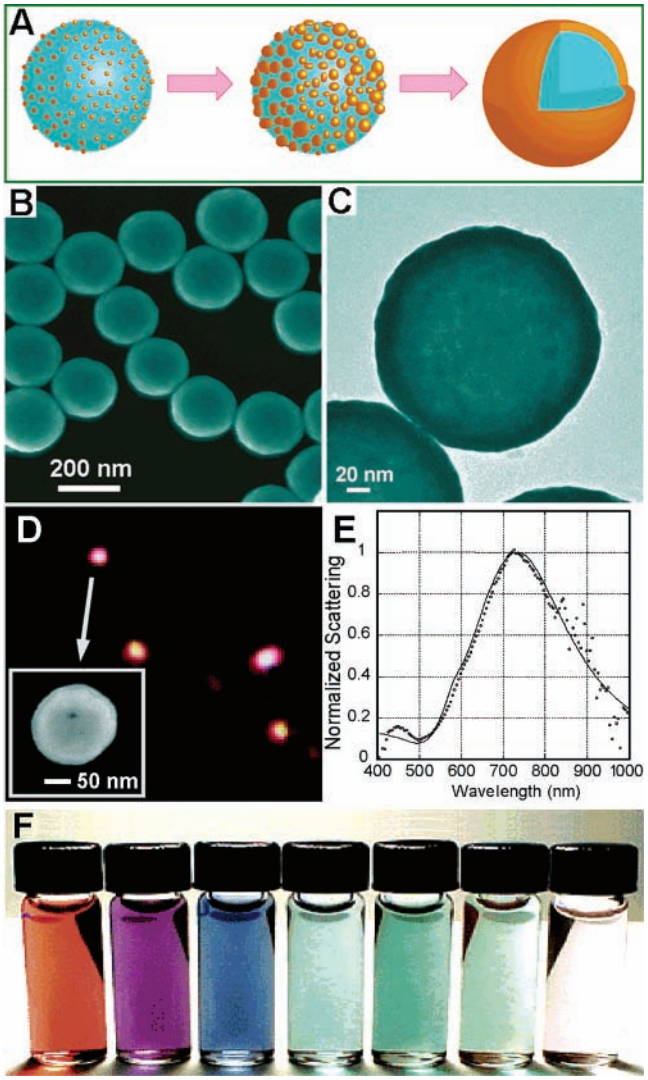

FIGURE 3. (A) Schematic illustration of the silica−Au nanoshell fabrication, (B) SEM and (C) TEM images of experimentally fabricated nanoshells, (D) dark-field image of nanoshells dispersed on ITO with an inset showing a SEM image of the individual nanoshell indicated by arrow, (E) single-particle scattering spectrum of the nanoshell in panel D and calculated scattering spectrum of a nanoshell of geometry $[r_1,r_2] = [60,80]$ nm using Mie scattering theory, and (F) vials containing aqueous solutions of (left-most vial) solid Au nanospheres and silica−Au nanoshells.

tetrachloroauric acid in the presence of sulfide ions, which leads to the formation of a Au_2S core followed by a crystalline outer Au shell layer, as established by optical measurements of the nanoparticle resonant response during growth.[8,22] Another successful synthesis consists of a reduction of Au onto a solid Ag nanoparticle core followed by electrochemical dissolution of the Ag core.[23] In our work, a sequential growth method has been developed that permits the independent synthesis of the core and shell layers of the nanoshell structure. This approach allows for a greater control over the monodispersity of both the core and the product nanoshell with both high purity and high yield of the desired nanostructure.[9] A schematic illustrating the sequential growth method is shown in Figure 3A. The first step involves the

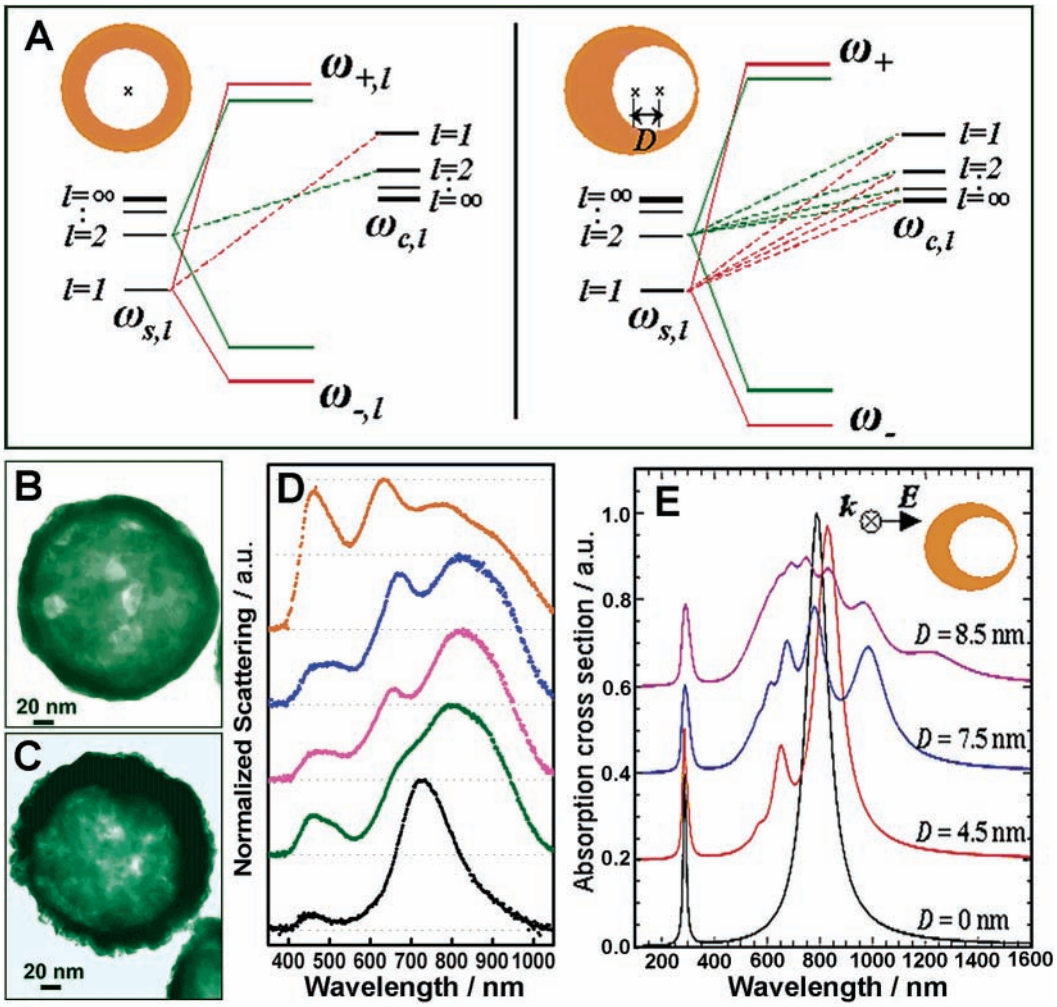

FIGURE 4. (A) Schematic of plasmon hybridization in a nanoshell (left) and a nonconcentric nanoshell or "nanoegg" (right), TEM images of (B) a nanoshell and (C) a nanoegg, (D) normalized single-particle dark-field scattering spectra of a nanoshell (black [*a*, *b*] = 94, 103 nm) and four different individual nanoegg particles with different core offsets (colored spectra), and (E) theoretical absorption spectra as function of offset *D* obtained by the plasmon hybridization method for [*a*, *b*] = 39, 48 nm Au nanoshell with a vacuum core.

functionalization of silica nanoparticle cores with aminopropyltrimethoxysilane. This terminates the silica nanoparticle with an amine-rich layer, which allows the anchoring of ultrasmall (1−2 nm diameter) Au islands onto the Au surface. Further Au is reduced onto this parent structure until a complete metallic shell layer is formed (Figure 3B,C). The shell thickness can be precisely controlled by adjusting the amount of Au deposited on the surface of the silica nanoparticles. Nanoshells fabricated by this method have excellent correspondence between experimental and theoretical plasmon resonance frequency (Figure 3D,E).

Nanoeggs

The plasmon hybridization picture has been applied to the case of a nanoshell with an offset core, reduced-symmetry nanoshells that we have termed "nanoeggs" (Figure 4).[10] For spherical nanoshells, plasmon hybridization occurs only between cavity and sphere plasmon states of the same multipolar index, denoted by *l*. However, when the center of the inner shell radius is displaced with respect to the center of the outer shell radius, this selection rule is relaxed, and cavity and sphere plasmons of all multipolar indices hybridize (Figure 4A). As a consequence, all plasmon modes of this structure can be optically excited, even in the dipole limit, resulting in a strongly multipeaked and red-shifted plasmonic response that increases in structure and complexity with increasing core−shell displacement, *D*.

Nanoeggs are experimentally fabricated by anisotropically depositing additional metallic Au onto already fabricated silica−Au concentric nanoshells (Figure 4B,C). The Au nanoshells are first immobilized onto poly(vinyl pyridine)-functionalized glass substrates as a monolayer of isolated nanoshells. The nanoshell films are subsequently immersed in an aqueous solution containing an appropriate amount of chloroauric acid and potassium carbonate, where the addition of formaldehyde then initiates the electroless plating of Au onto the nanoparticle surfaces. The films are subsequently removed from the plating solution, rinsed, and dried. As a result, all the nanoeggs fabricated in this manner have the same orientation on the glass slides, with the point of contact with the glass substrate corresponding to the minimum in shell

thickness for each nanoparticle. Increasing the time duration of the plating process results in an increase in the effective core offset of each nanoegg particle. As the offset between the center of the inner and outer shell radius increases, the optical spectrum broadens and includes additional peaks adjacent to the original dipolar plasmon resonance, revealed in the single-particle UV–visible spectra of individual nanoeggs of increasing asymmetry (Figure 4D,E). The experimentally obtained optical spectra of the individual nanoegg particles clearly show this characteristic offset-dependent multipeaked spectrum.

Nanomatryushkas

This structure is a concentric nanoshell composed of a dielectric core with alternating layers of metal, dielectric, and metal, essentially a nanoshell encased within another nanoshell, inspiring its alternative Russian name of "nanomatryushka" (Figure 5).[5,11] The plasmon response of this structure can be understood as a hybridization of the plasmon resonances of the inner and outer nanoshells. As illustrated in Figure 5A, for each multipolar symmetry, there are four linearly independent, incompressible charge deformations (plasmons). The interaction results in four hybridized plasmon resonances. The thickness of the dielectric spacer layer, $|a_2 - b_1|$, controls the strength of the coupling between the inner and the outer nanoshell, whose plasmon resonances can each be tuned independently. The resulting plasmon resonances are in exact agreement with classical Mie scattering theory.

The nanomatryushka geometry can be experimentally realized by first growing a uniform nanoscale layer of gold around a silica nanoparticle core, then coating this nanoparticle with a silica layer of controlled thickness, followed by a second thin shell layer of gold (Figure 5B).[5,11] Figure 5C shows the hybridized plasmon response of concentric nanoshells for the case of strong hybridization between the inner and outer metallic shell layers. Spectrum 1 shows the experimental and theoretical extinction spectrum for the isolated inner shell plasmon $|\omega_{-,NS_1}\rangle$. Spectrum 2 is the theoretical extinction spectrum of the isolated outer shell plasmon $|\omega_{-,NS_2}\rangle$, calculated as though the inner shell structure was replaced wholly by a dielectric (silica) core. Spectrum 3 is the experimental and theoretical extinction for the concentric nanoshell: here the $|\omega^{+}_{-,CS}\rangle$ and $|\omega^{-}_{-,CS}\rangle$ plasmons are clearly apparent.

Nanorice

This hybrid nanoparticle combines the tunable plasmonic characteristics of nanorods and nanoshells into a single geometry.[12] A nanorice particle is composed of a spindle-shaped, nonmagnetic hematite core coated with a continuous nanometer-thick Au shell (Figure 6A). This dielectric core–metallic shell prolate spheroid nanoparticle bears a remarkable resemblance to a grain of rice, inspiring the name "nanorice" (Figure 6B). The fabrication of nanorice involves seeded metallization of spindle-shaped hematite nanoparticle cores. Small Au nanoparticles (~2

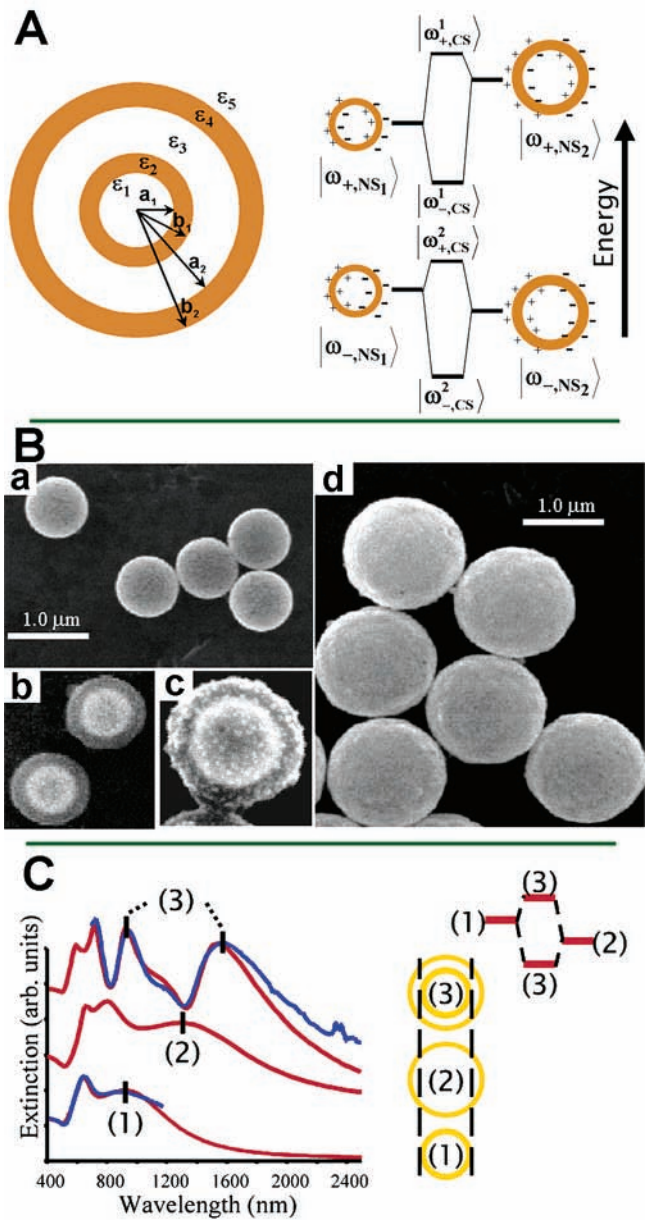

FIGURE 5. (A) Concentric nanoshell geometry (left) with concentric radii of core (a_1), inner shell (b_1), spacer layer (a_2), and outer shell (b_2) where ϵ_1 and ϵ_3 are assumed to be SiO_2, ϵ_2 and ϵ_4 are Au, and ϵ_5 is embedding medium and energy level diagram (right) of the hybridization of the inner and outer nanoshell plasmons in this structure, (B) SEM images of (a) inner nanoshell, consisting of a silica core layer and a gold shell layer of 800 nm total diameter, (b) silica encapsulated core (235 nm silica layer), (c) seeded silica-coated nanoshell with Au colloid, and (d) complete concentric nanoshell with total particle diameter 1.4 μm, and (C) experimental (blue) and theoretical (red) extinction spectra for concentric nanoshells (3) and inner (1) and outer (2) nanoshell plasmon resonances for a geometry with strong hybridization between inner and outer nanoshell plasmon. Peak positions in spectra are marked for clarity. The theoretical extinction spectra were calculated using Mie scattering theory.

nm in diameter) are immobilized onto the surface of aminopropyltrimethoxysilane functionalized cores at a nominal coverage of ~30%. The immobilized Au colloids act as nucleation sites for electroless Au plating onto the surface of core particles, leading to the gradual formation

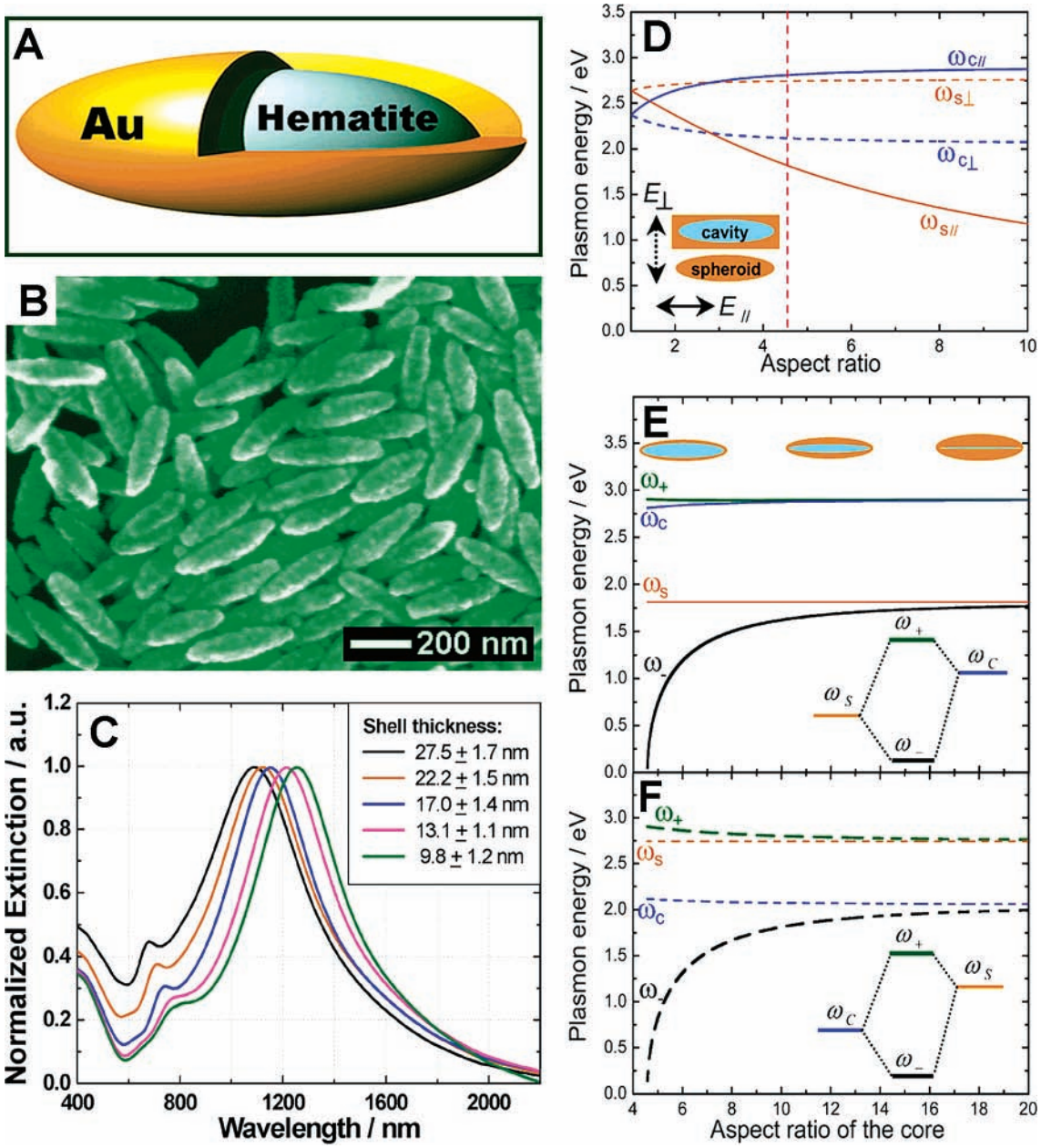

FIGURE 6. (A) Illustration of nanorice, (B) SEM image, (C) extinction spectra of nanorice longitudinal plasmon ~1200 nm with different shell thicknesses as particles dispersed and immobilized on poly(vinyl pyridine)-coated glass slides, fabricated on a hematite core with longitudinal diameter of 340 ± 20 nm and transverse diameter of 54 ± 4 nm, (D) plasmon energy vs aspect ratio (major radius/minor radius) of the solid prolate spheroid and prolate cavity (solid lines, longitudinal plasmon; dashed lines, transverse plasmon), and (E) longitudinal and (F) transverse plasmon energies vs core aspect ratio for an aspect ratio of 4.575. The orange and blue lines indicate the plasmon energies of the solid prolate spheroid and the prolate cavity modes, respectively. The black and green lines refer to bonding (ω_-) and antibonding (ω_+) plasmons, respectively.

of a continuous and complete Au shell layer. Within this hybrid nanoparticle geometry, we see that the plasmon tunability arising from varying the thickness of the shell layer is far more geometrically sensitive than that arising from varying the ellipticity of the solid parent nanostructures (Figure 6C).

To apply the plasmon hybridization picture to analyze the resonances of this layered nanoparticle geometry, we analyze the plasmon resonances of a solid metallic nanospheroid and a nanocavity of arbitrary ellipticity (Figure 6D). These are the two structures that support the parent plasmons, which, when hybridized, give rise to the transverse and longitudinal plasmon resonances of nanorice (Figure 6E,F). This is a generalization of the sphere–cavity model to spheroidal structures of arbitrary ellipticity. In Figure 6D, we show the dependence on aspect ratio of the transverse and longitudinal plasmon resonances of a Au spheroid and that of an elliptical hematite cavity embedded in an infinite Au volume.

The reason why the cavity modes have lower energy for aspect ratio = 1 than the solid particle modes is the large dielectric permittivity of the hematite core. Each of these nanostructures supports longitudinal and transverse plasmon resonances strongly dependent upon aspect

ratio. As the aspect ratio increases, the energies of the longitudinal plasmon of the solid spheroid and the transverse plasmon of the cavity decrease, while the energy of the longitudinal plasmon of the cavity and the transverse plasmon of the spheroid increases. Varying the aspect ratio of the cavity and spheroid significantly shifts the relative energy of the cavity and spheroid parent plasmon modes, which ultimately affects the way in which the cavity and spheroid plasmon states hybridize in the nanorice geometry.

Figure 6E,F shows the longitudinal and transverse plasmon frequencies of nanorice as a function of the aspect ratio of the core for a fixed outer aspect ratio of 4.575, which corresponds to the experimentally realized nanorice (denoted by the dashed vertical red line in Figure 6D). The nanorice plasmon resonances shift as the aspect ratio of the core is varied. As the aspect ratio of the core decreases, the hybridization between the cavity and spheroid modes becomes progressively stronger, resulting in larger energy gaps between the bonding and antibonding plasmon modes. The lower energy "bonding" plasmon modes of nanorice are much more sensitive to the core and shell dimensions than the "antibonding" plasmon modes for both the longitudinal and the transverse case. In particular, the "bonding" plasmon extends toward zero frequency in the thin shell limit for both the transverse and longitudinal case. For longitudinal polarization, the nature of the bonding plasmon is solid-particle-like and that of the antibonding mode is cavity-like. For transverse polarization, the situation is reversed. Only the solid-particle-like plasmons couple strongly to incident light.

Multiparticle Plasmons: Dimers, Trimers, Quadrumers, etc.

An important topic in the field of nanophotonics is how the plasmon modes of nanoparticles change in the presence of other plasmonic particles. Plasmon hybridization allows us to express the fundamental plasmon modes of multi-nanoparticle systems as linear combinations of plasmons of individual nanoparticles, in a manner analogous to molecular orbital theory.

The defining characteristic of the plasmon hybridization picture of systems of nanoparticle assemblies is the interaction of a multipolar plasmon of one particle with all other multipolar plasmons of the other particles.[13−15] The term describing an interaction between the multipole (l,m) on particle i with (l',m') on particle j is given by

$$I^{i,j}_{l,m,l',m'}(R) = \frac{1}{R^2}\int \frac{Y_{l,m}(\Omega_i)Y_{l',m'}(\Omega_j)}{r_j^{l'+1}}\,\mathrm{d}S_i$$

where the integration is centered on particle i and done over its radius R. The quantity r_j is the distance from the center of a separate particle j to a point on this surface. Subscripts on Ω denote on which particle the coordinate is centered. This term can be evaluated analytically using the addition theorem of solid harmonics.[24] The result gives a distance relation that depends on $1/D^{l+l'+1}$ where D is the center to center separation of the two particles.

Due to the interaction of multipolar plasmons, the plasmons of a multiparticle structure will in general have a mixed multipolar composition. In particular, dipole components mix into modes that are $l = 2$ or higher in the absence of such interactions. The dipole components mix into the higher modes with the same symmetry that they possess in the absence of interactions. For dimers, the dipole plasmon modes can be categorized into those parallel and perpendicular to the dimer axis and in aligned or anti-aligned combinations. For a homodimer, the excitable parallel modes are bonding plasmons and shift to lower energies with decreasing dimer separation, while the excitable perpendicular plasmon modes are antibonding, shifting to higher energies with decreasing particle separation. For a heterodimer (Figure 7) both the bonding and antibonding modes for both polarizations can be excited by light.

Because of the invariance of the interactions through symmetry transformations for a specific structure, group theory may be applied quite naturally to this analysis (Figure 8). Symmetric linear combinations of plasmons corresponding to the underlying symmetry of the system were used to interpret and classify the modes of a nanosphere trimer (group D_{3h}) and quadrumer (group D_{4h}).[15] These linear combinations were used to predict which modes have a dipole moment for a given polarization and resulted in a significant simplification of the problem. For the trimer, only E′ modes are visible for in-plane excitations, and only A_2'' modes are visible for out-of-plane excitations (Figure 8). For the quadrumer, E_u modes are visible for the in-plane excitations, and A_{2u} modes are visible for the out-of-plane excitations. In both cases, the in-plane modes shift to lower energies with decreasing nanoparticle separation, while the out-of-plane modes shift to higher energies with decreasing separation.

Nanoparticle on a Film: The Plasmonic Anderson Model

The discrete, localized plasmon resonances of a metallic nanoparticle can also interact with the continuum of surface plasmons of a semi-infinite surface or a metallic film.[16,25] Such plasmon hybridization between a metallic nanoparticle and an extended metallic structure can be regarded as an electromagnetic analog of the spinless Anderson−Fano model,[26−28] the standard model used to describe the interaction of a localized state with a continuum of delocalized states.

The interaction of metallic nanoparticles with adjacent conducting surfaces has been of long-standing interest in the context of plasmon propagation and near-field enhancement.[29−35] However, while the interaction between the nanoparticle plasmon and the film plasmon is dependent on particle−substrate separation (Z),[29,35−38] it can also be controlled by the thickness of the underlying metallic film substrate. For a discrete state interacting with a continuum, the parameter determining the nature of the resulting states is the effective continuum $\rho(\omega)V^2(\omega)$, where $\rho(\omega)$ is the density of states of the continuum and $V(\omega)$ is

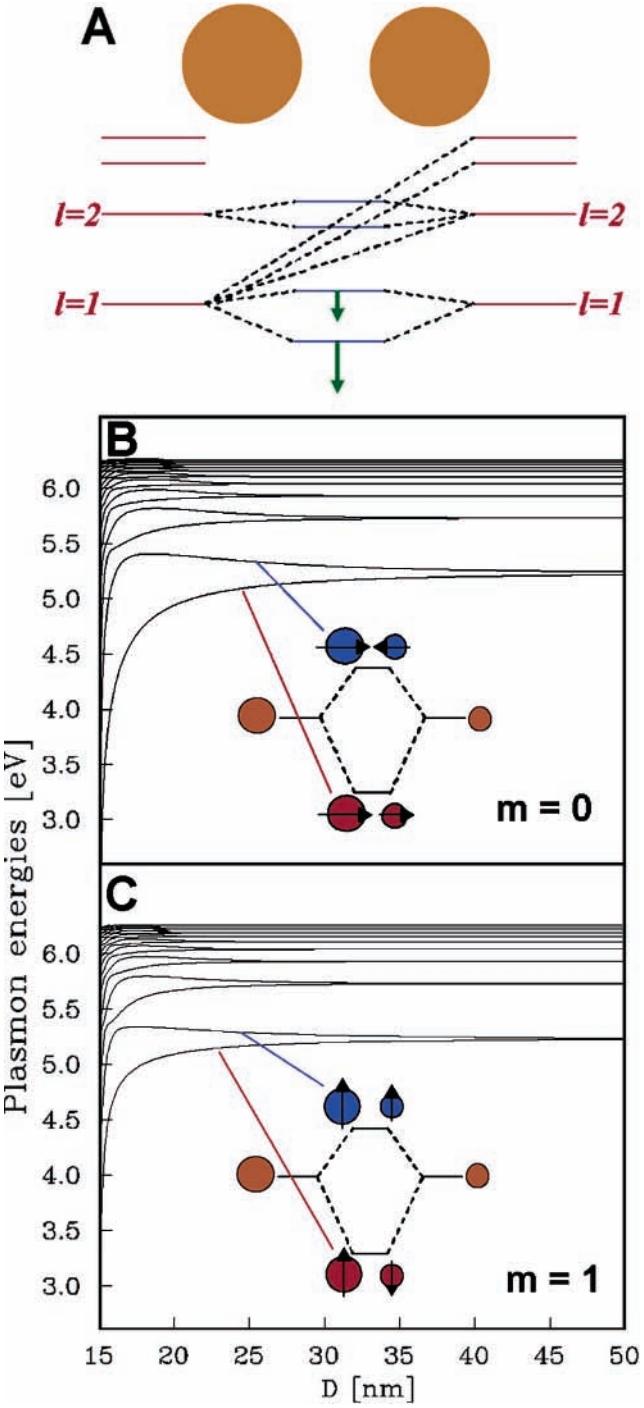

FIGURE 7. (A) Schematic diagram of the dimer system and calculated plasmon energies vs dimer separation for a heterodimer composed of 10 and 5 nm spheres for (B) parallel and (C) perpendicular polarization. Insets are schematics of the dipolar interaction and the resulting dipole combinations for each polarization. The plasmons of heterodimers exhibit avoided crossings because of broken symmetry.

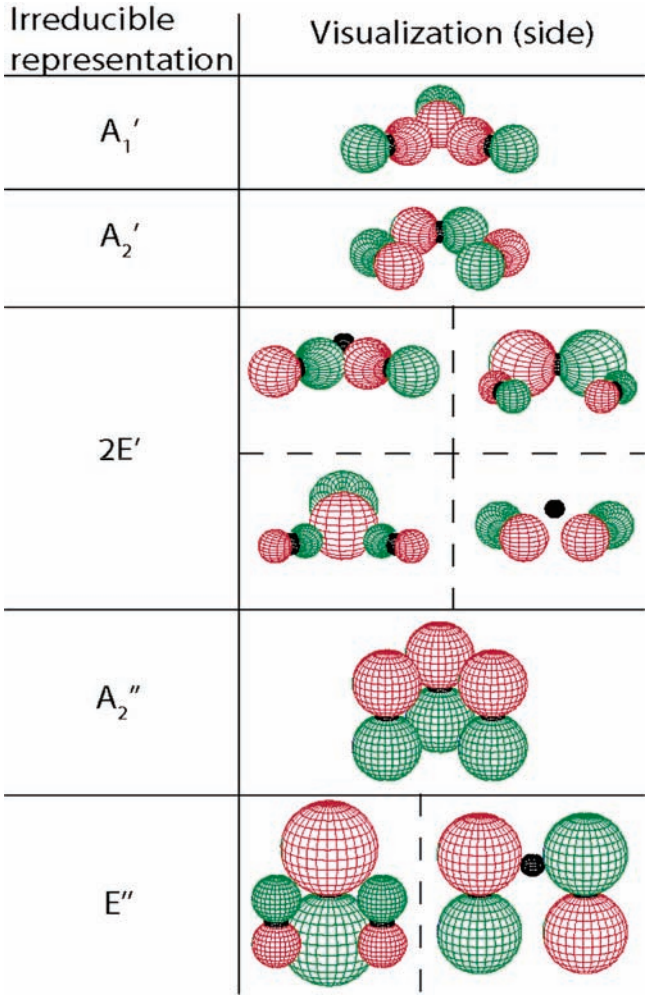

FIGURE 8. Dipolar symmetry-adapted basis sets for a trimer derived using group theory. The dipolar component of the plasmons associated with one-dimensional representations is shown exactly, and the dipolar component of the physical plasmons associated with two-dimensional representations is a linear combination of the corresponding basis sets.

the coupling between the discrete state and a continuum mode of energy ω. For a metallic film of finite thickness, the effective continuum is a thickness-dependent continuous function of energy ranging from zero to the bulk plasmon energy.[16]

The interaction regimes between the discrete plasmon level of the nanoparticle and the continuum of surface plasmon states of the metallic film are shown schematically in Figure 9. Here the three distinct regimes of interaction are depicted. As in the quantum impurity models, the interaction can result both in virtual resonances at energies in the continuum and in localized states at energies outside the continuum, that is, above or below the band, depending on the continuum parameters. In the thick film case ($T > 2Z$), illustrated in Figure 9B, the effective film continuum lies above the nanosphere plasmon energy. In this case, the effective continuum is extremely narrow and the surface plasmon density of states is highly degenerate. Hybridization between the localized sphere plasmons and the sharp distribution of surface plasmons around ω_{sp} results in strong, localized, low-energy "bonding" and higher energy "antibonding" states. This is qualitatively similar to the hybridization of a nanosphere outside a semi-infinite surface.[25] For intermediate film thicknesses ($T \approx Z$), the nanosphere plasmon energies lie within the effective surface plasmon continuum (Figure 9C). In this regime, the interaction results in resonances, that is, a broadening of the discrete

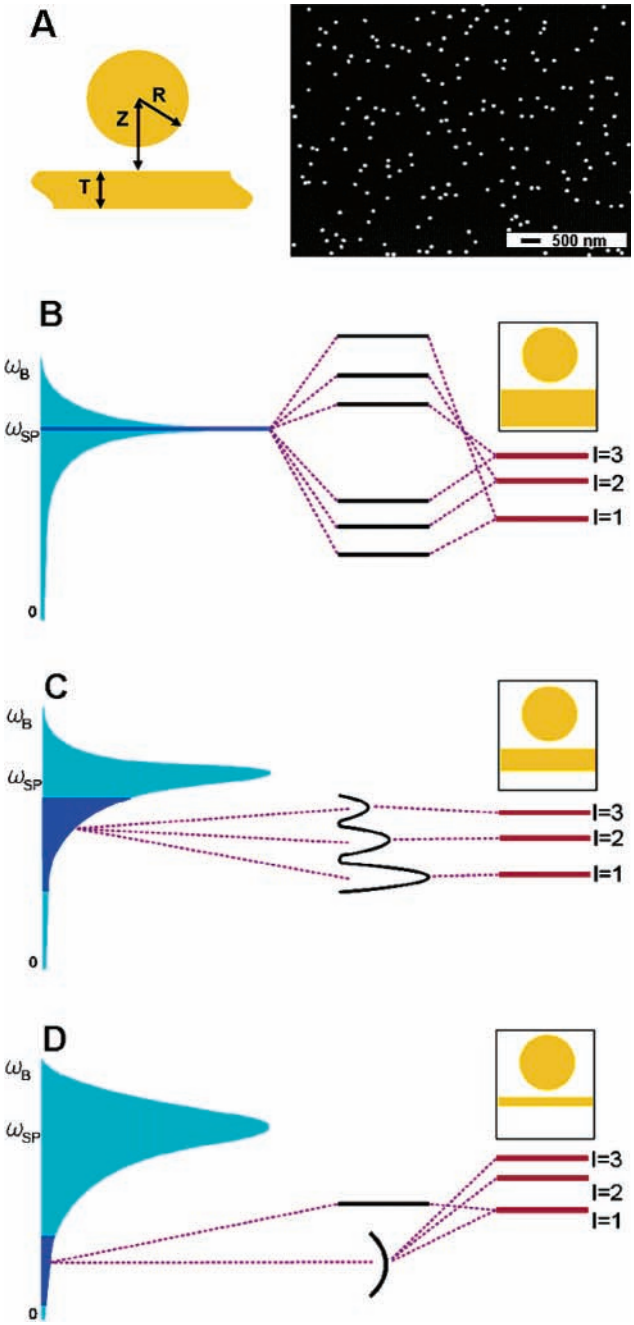

FIGURE 9. (A) Schematic (left) depicting the geometrical parameters of the interacting nanoparticle and film and SEM image (right) of representative experimental sample consisting of dispersed Au nanoparticles on a thin Au film and (B−D) schematics illustrating the three regimes of interaction for the plasmonic continuum of a conducting film (left) with the discrete plasmons of a nanosphere (right): (B) "thick film" ($T > 2Z$); (C) intermediate film thickness ($T \approx Z$); (D) "thin film" ($T < Z/2$). The interactions between nanosphere and thin film plasmons are determined by the effective continuum ρV^2 (dark blue) where $\rho(\omega)$ is the plasmon density of states of the film (light blue) and $V(\omega)$ is the interaction between a nanosphere plasmon and a film plasmon of energy ω. Insets show geometries to approximate scale.

nanoparticle plasmons due to their possibility of transfer into the film. In the thin film regime ($T < Z/2$), the effective film continuum lies at lower energies than the discrete plasmons of the nanosphere (Figure 9D). The high-energy hybridized plasmon is a localized state above the continuum and remains narrow: it is composed primarily of the discrete nanoparticle plasmon resonances. The broad low-energy feature illustrated by the arc is a virtual resonance in the continuum. The virtual state is composed of delocalized film plasmons of energies within the effective continuum of surface plasmon states.

Experimentally, the thin film regime is the regime that can be probed most straightforwardly by performing optical transmission measurements on thin film−nanoparticle samples. The samples for experimental measurements were constructed by immobilizing isolated Au nanospheres on PVP-functionalized Au thin films (Figure 9). In the thin film regime, two hybridized plasmon resonances are observed: a higher-energy resonance corresponding to the localized state above the continuum and a lower energy feature corresponding to the virtual state in the continuum. The experimental observations are in excellent agreement with the theoretical simulations.

Concluding Remarks

We have presented a conceptually simple and intuitive picture that allows us to understand plasmons supported by simple geometries and to predict the plasmon resonant properties of geometries of increasing complexity. The plasmon modes of a metallic nanostructure are a mesoscale analog of molecular orbital theory, hybridizing in precisely the same manner as individual atomic wave functions in molecules. Applying the plasmon hybridization model as a design principle to experimentally realizable nanostructures provides a powerful platform for the selective implementation of optimized optical properties into structures and devices of mesoscale dimensions, enabling widespread applications in optical nanodevice construction, ultrasensitive molecular sensing, and biomedicine.

We gratefully acknowledge the National Science Foundation, the Air Force Office of Scientific Research, the Army Research Office, the National Aeronautics and Space Administration, and the Robert A. Welch Foundation for financial support.

References

(1) Mie, G. Beitrage zur Optik trüber Medien, speziell kolloidaler Metallosungen. *Ann. Phys.* **1908**, *25*, 377−452.
(2) Halperin, W. P. Quantum size effects in metal particles. *Rev. Mod. Phys.* **1986**, *58* (3), 533−606.
(3) Kreibig, U.; Vollmer, M. *Optical Properties of Metal Clusters*; Springer-Verlag: Berlin, 1995.
(4) El-Sayed, M. A. Some interesting properties of metals confined in time and nanometer space of different shapes. *Acc. Chem. Res.* **2001**, *34*, 257−264.
(5) Prodan, E.; Radloff, C.; Halas, N. J.; Nordlander, P. A hybridization model for the plasmon response of complex nanostructures. *Science* **2003**, *302*, 419−422.
(6) Steigerwald, M. L.; Brus, L. E. Semiconductor crystallites: A class of large molecules. *Acc. Chem. Res.* **1990**, *23*, 183−188.
(7) Alivisatos, A. P. Semiconductor clusters, nanocrystals, and quantum dots. *Science* **1996**, *271*, 933−937.
(8) Averitt, R. D.; Sarkar, D.; Halas, N. J. Plasmon resonance shifts of Au-coated Au2S nanoshells: Insight into multicomponent nanoparticle growth. *Phys. Rev. Lett.* **1997**, *78* (22), 4217−4220.
(9) Oldenburg, S. J.; Averitt, R. D.; Westcott, S. L.; Halas, N. J. Nanoengineering of optical resonances. *Chem. Phys. Lett.* **1998**, *288* (2−4), 243−247.

(10) Wang, H.; Wu, Y.; Lassiter, B.; Nehl, C.; Hafner, J. H.; Nordlander, P.; Halas, N. J. Symmetry-breaking of individual plasmonic nanoparticles. *Proc. Natl. Acad. Sci. U.S.A.* 2006, *103*, 10856−10860.
(11) Radloff, C.; Halas, N. J. Plasmonic properties of concentric nanoshells. *Nano Lett.* **2004**, *4*, 1323−1327.
(12) Wang, H.; Brandl, D. W.; Le, F.; Nordlander, P.; Halas, N. J. Nanorice: a hybrid plasmonic nanostructure. *Nano Lett.* **2006**, *6* (4), 827−832.
(13) Nordlander, P.; Oubre, C.; Prodan, E.; Li, K.; Stockman, M. I. Plasmon hybridization in nanoparticle dimers. *Nano Lett.* **2004**, *4*, 899−903.
(14) Brandl, D. W.; Oubre, C.; Nordlander, P. Plasmon hybridization in nanoshell dimers. *J. Chem. Phys.* **2005**, *123*, No. 024701.
(15) Brandl, D. W.; Mirin, N. A.; Nordlander, P. Plasmon modes of nanosphere trimers and quadrumers. *J. Phys. Chem. B* **2006**, *110*, 12302−12310.
(16) Le, F.; Lwin, N. Z.; Steele, J. M.; Kall, M.; Halas, N. J.; Nordlander, P. Plasmons in the metallic nanoparticle - Film system as a tunable impurity problem. *Nano Lett.* **2005**, *5* (10), 2009−2013.
(17) Prodan, E.; Nordlander, P.; Halas, N. J. Effects of dielectric screening on the optical properties of metallic nanoshells. *Chem. Phys. Lett.* **2003**, *368* (1−2), 94−101.
(18) Prodan, E.; Nordlander, P. Electronic structure and polarizability of metallic nanoshells. *Chem. Phys. Lett.* **2002**, *352* (3−4), 140−146.
(19) Prodan, E.; Nordlander, P. Structural tunability of the plasmon resonances in metallic nanoshells. *Nano Lett.* **2003**, *3* (4), 543−547.
(20) Prodan, E.; Nordlander, P.; Halas, N. J. Electronic structure and optical properties of gold nanoshells. *Nano Lett.* **2003**, *3*, 1411−1415.
(21) Prodan, E.; Nordlander, P. Plasmon hybridization in spherical nanoparticles. *J. Chem. Phys.* **2004**, *120* (11), 5444−5454.
(22) Zhou, H. S.; Honma, I.; Komiyama, H.; Haus, J. W. Controlled synthesis and quantum-size effect in gold-coated nanoparticles. *Phys. Rev. B* **1994**, *50* (16), 12052−12056.
(23) Sun, Y. G.; Xia, Y. N. Increased sensitivity of surface plasmon resonance of gold nanoshells compared to that of gold solid colloids in response to environmental changes. *Anal. Chem.* **2002**, *74* (20), 5297−5305.
(24) Chakrabarti, S.; Dewangan, D. P. Addition theorems for solid harmonics and the second Born amplitudes. *J. Phys. B: At., Mol. Opt. Phys.* **1995**, *28*, L769−L774.
(25) Nordlander, P.; Prodan, E. Plasmon hybridization in nanoparticles near metallic surfaces. *Nano Lett.* **2004**, *4* (11), 2209−2213.
(26) Anderson, P. W. Localized magnetic states in metals. *Phys. Rev.* **1961**, *124* (1), 41.
(27) Fano, U. Effects of configuration interaction on intensities and phase shifts. *Phys. Rev.* **1961**, *124* (6), 1866.
(28) Mahan, G. D. *Many-Particle Physics*; Kluwer Academic/Plenum Publishers: New York, 2000.
(29) Stuart, H. R.; Hall, D. G. Enhanced dipole-dipole interaction between elementary radiators near a surface. *Phys. Rev. Lett.* **1998**, *80* (25), 5663−5666.
(30) Lamprecht, B.; Schider, G.; Lechner, R. T.; Ditlbacher, H.; Krenn, J. R.; Leitner, A.; Aussenegg, F. R. Metal nanoparticle gratings: Influence of dipolar particle interaction on the plasmon resonance. *Phys. Rev. Lett.* **2000**, *84*, 4721−4724.
(31) Linden, S.; Kuhl, J.; Giessen, H. Controlling the interaction between light and gold nanoparticles: Selective suppression of extinction. *Phys. Rev. Lett.* **2001**, *86*, 4688−4691.
(32) Maier, S. A.; Kik, P. G.; Atwater, H. A.; Meltzer, S.; Harel, E.; Koel, B. E.; Requicha, A. G. Local detection of electromagnetic energy transport below the diffraction limit in metal nanoparticle plasmon waveguides. *Nat. Mater.* **2003**, *2*, 229−232.
(33) Lal, S.; Westcott, S. L.; Taylor, R. N.; Jackson, J. B.; Nordlander, P.; Halas, N. J. Light interaction between gold nanoshells plasmon resonance and planar optical waveguides. *J. Phys. Chem. B* **2002**, *106* (22), 5609−5612.
(34) Larkin, I. A.; Stockman, M. I.; Acherman, M.; Klimov, V. I. Dipolar emitters at nanoscale proximity of metal surfaces: Giant enhancement of relaxation in microscopic theory. *Phys. Rev. B* **2004**, *69*, No. 121403.
(35) Aravind, P.; Metiu, H. The effects of the interaction between resonances in the electromagnetic response of a sphere-plane structure; applications to surface enhanced spectroscopy. *Surf. Sci.* **1983**, *124*, 506−528.
(36) Okamoto, T.; Yamaguchi, I. Optical absorption study of the surface plasmon resonance in gold nanoparticles immobilized onto a gold substrate by self-assembly technique. *J. Phys. Chem. B* **2003**, *107* (38), 10321−10324.
(37) Gozhenko, V. V.; Grechko, L. G.; Whites, K. W. Electrodynamics of spatial clusters of spheres: Substrate effects. *Phys. Rev. B* **2003**, *68* (12), No. 125422.
(38) Pinchuk, A.; Hilger, A.; von Plessen, G.; Kreibig, U. Substrate effect on the optical response of silver nanoparticles. *Nanotechnology* **2004**, *15* (12), 1890−1896.

AR0401045